Journal of Hazardous Materials 419 (2021) 126485

Contents lists available at ScienceDirect

Journal of Hazardous Materials

journal homepage: www.elsevier.com/locate/jhazmat

Highly efficient and recyclable polyolefin-based magnetic sorbent for oils and organic solvents spill cleanup

Hyeongoo Kim [a], Gang Zhang [b], Min Wu [c], Jinshan Guo [c], Changwoo Nam [a,*]

[a] Organic Materials and Fiber Engineering, Jeonbuk National University, 567 Baekje-daero, Deogjin-dong, Deokjin-gu, Jeonju, Jeollabuk-do 54896, Republic of Korea
[b] Department of Materials Science and Engineering, The Pennsylvania State University, University Park, PA 16802, United States
[c] Department of Histology and Embryology, School of Basic Medical Sciences, Southern Medical University, Guangzhou 510515, China

ARTICLE INFO

Editor: Dr. H. Artuto

Keywords:
Polyolefin
Oil spill
Magnetic nanoparticle
Sorbent
Oil recycling

ABSTRACT

The oil dispersants have been applied in a broad oil pollution area, but the dispersed oil caused environmental problems during sedimentation. Unlike oil dispersants, flake type polyolefin-based oil absorbent (PA) is not emulsified and shows excellent swelling characteristic for oil removal. However, the sprayed PA flakes cannot be fully collected due to its tiny architectures, the uncollected flakes can cause unintentional secondary pollution. In this study, we develop a kind of flake type polyolefin-based magnetic absorbent (PMA) hybridized with magnetic nanoparticle, to facilitate the collection process. The magnetic nanoparticle is uniformly dispersed in PMA due to the hydrophobic functionalization of iron oxide nanoparticle. This enables the convenient collection of isolated sorbent flakes even when they were placed in the marine system and show a desirable oil recovery performance up to about 37 times for organic solvent. Moreover, oil-soaked PMA flakes can be fully converted into refined oil via a pyrolysis process. After pyrolysis, the thermally undecomposed compounds, which comprise of carbon residue and magnetic nanoparticle, can be also separated by a magnet. The as-prepared flake type PMA possesses good oil recovery performance, fast magnetic response, and efficient oil recycling, thus representing an environmentally promising method for oil spill cleanup.

1. Introduction

Large-scale oil spill requires prompt action for reducing the impacts on the ocean environment and needs proper methods for cleaning up the broad liquid pollutant region (Ivshina et al., 2015; Romero et al., 2017; Yim et al., 2012). Chemical dispersants mainly constitute more than half of large-scale oil spill remediation. In current technology, a chemical dispersant is one of the practical approaches that are available to respond to remote and large-scale oil spills in the ocean (Prince, 2015). However, the chemical dispersant can be limited by sea condition, high cost, and their high toxicity to aquatic organisms (Almeda et al., 2018; Dave, 2011; Karatepe, 2003; Kleindienst et al., 2015). Because of oil and chemical spills still releasing large volumes into the sea and the need for minimizing the formation of secondary pollution, one promising solution to large scale oil removal without pollution is converted a normal sorbent into functionalized sorbent with large sorption capacity and are easy to recover from the oil/water mixture. Oil sorbents are inexpensive and readily available in large quantities that can offer a quick method and a useful resource in response to a small-scale incident where a small volume of oil forms a spill area (Asadpour et al., 2013; Ge et al., 2016). However, oil sorbents are not useful to respond to massive oil or chemical spills in the open sea that cannot be reached by oil sorbents. Most conventional oil sorbents have macroscopic 3-dimensional (3D) structures such as pad, roll, and sponge, and they are generally used during the final stages of shoreline cleanup and recovering small pools of oil (Chen et al., 2021; Gui et al., 2010; Yu et al., 2013). Thus, as an alternative to cover a broad oil contaminated area, there has been a demand for a flake type oil sorbent capable of being sprayed and floating on the water surface. After polymerization, benefiting from the elastic characteristics, the synthesized oil sorbent can be produced into several forms, such as film, foam, and flake using flexible fabrication method (Gao et al., 2017; Nam et al., 2018a, 2018b, 2018c; G. Wang et al., 2020). Besides, adding semi-crystalline linear low-density polymer to amorphous low-crosslinked polymer (LCP), which cause absorbing abundant oil molecules to the polymer matrix, allows the production of interpenetrated polymeric oil sorbent (Shen et al., 2017). Flake type oil sorbent from LCP can be potentially used in broad oil pollutant region with the help of airplane or air sprayer (Nam et al., 2018a, 2018b,

* Corresponding author.
E-mail address: cun120@jbnu.ac.kr (C. Nam).

https://doi.org/10.1016/j.jhazmat.2021.126485
Received 9 March 2021; Received in revised form 7 June 2021; Accepted 22 June 2021
Available online 27 June 2021

2018c).

Among the thermoplastic deformation elastomers, polyolefins are promising materials that meet all the above criteria for large-scale oil spill cleanup (Yuan and Chung, 2012). Polyolefins, such as polypropylene (PP) and polyethylene (PE), are macromolecules synthesized by the polymerization of olefin monomer units, are prevalent in a wide array of applications depending on the characteristics of the polymer (Chung, 2013; Kaminsky, 1996; Zhang et al., 2017, 2018). Furthermore, polyolefins are composed of chemical hydrocarbons with oil likeness characteristic nature, thus have effective application as an oil sorbent (Takuma et al., 2001). In contrast to the porous sorbents (Wu et al., 2012), such as metal-organic framework (MOF) (Gu et al., 2019), and carbon-based sorbents (Fuller and Bonner, 2001; Gui et al., 2011, 2010; Sun et al., 2013; H. Wang et al., 2020; Zhu et al., 2013), low-crosslinked polyolefin-based sorbent shows oil swelling behaviors in polyolefin networks with increased volume (Guvendiren et al., 2009; Nam et al., 2016a, 2016b, 2018a, 2018b, 2018c). The penetrating oil molecules are not able to escape from the network, they are continuously stored inside the sorbent matrix and lead to volume expansion (Kizil and Bulbul Sonmez, 2017; Ono et al., 2007). Furthermore, adding semi-crystalline polyolefin elastomer (POE) to LCP allows the abundant storage of oil molecules in the oil sorbent. After oil sorption, they contain essentially the same hydrocarbon mixtures presented in spilled oil. The small percentage of polymer content in the polyolefin-based adducts can be completely thermally decomposed into liquid hydrocarbon molecules at a temperature well below typical distillation temperature (~600 °C) during the first stage of the oil-refining process (Al Absi et al., 2020). However, sprayed polyolefin-based flakes are difficult to be fully collected from oil spill areas and require a power supplied equipment such as skimmer (Nam et al., 2018a, 2018b, 2018c). Furthermore, these flakes either lack sufficient collection, and have limited operating conditions due to high dispersity on water surface, or even require a boom and remained flakes in the ocean are possible to cause unintentional environmental pollution.

Magnetic separation is a convenient process used for decades in nearly all science areas. Because magnetic separation is very simple and the most conventional magnetic system only need to consist of a small permanent magnet (Singh et al., 2020), then we envisioned that magnetic nanoparticle could be used to collect whole flake type oil sorbents. Over the past reports, advanced oil sorbents with magnetic properties have been used in the limelight for the collection of oil recovered sorbents. Typically, carbon-based magnetic aerogels (Gui et al., 2013), biomass-derived magnetic sorbents (Graziele da Costa Cunha et al., 2019; Navarathna et al., 2020), functionalized sponges (Li et al., 2018; Liu et al., 2019), and magnetic nanoparticle sorbents (Sakti et al., 2021; Sarcletti et al., 2019) showed as several strengths such as high oil selectivity, massive oil sorption, and free control of oil sorbents under oil/water mixed system. Nevertheless, theses oil sorbents are impractical and remain limitations as they are not applicable in large-scale oil spills, they are also not able to suppress the massive oil pollutant at once. Therefore, inorganic-organic hybridized polyolefin-based magnetic oil sorbents are promising complementary material compared to the aforementioned oil sorbents.

In this study, we report a kind of polyolefin-based magnetic absorbent (PMA) with desirable swelling performance and magnetic property for spilled oil removal and efficient collection of the oil-soaked sorbents. This PMA was prepared from the polyolefin by interconnecting amorphous 1-decene/divinylbenzene (D/DVB) copolymer and semi-crystalline POE and blending with hydrophobic functionalized iron oxide nanoparticle (HIONP) (Fig. 1a). The PMA shows high swelling characteristic with good oil absorption due to its highly amorphous matrix. Furthermore, the deformed effective shape into flake oil sorbent can be applied in a broad oil spill region, and the magnet can simply collect the oil-soaked PMA flakes in the aqueous system. The collected oil-soaked PMA flakes can be fully converted into oil fuels, and the magnetic nanoparticles can be separated from the undecomposed compound after a pyrolysis process (Fig. 1b). In consequence, the advanced PMA flake provides a practical solution for fast oil spill remediation and large-scale oil spill.

2. Experimental section

2.1. Materials

All the monomers (1-decene and divinylbenzene (DVB) (purchased from the Merck, Republic of Korea)) for copolymerization were purified with CaH_2. Polyolefin elastomer (POE) (thermoplastic density: 0.865 g cm^{-3}, crystallinities: 12%, Engage®8180, purchased from Dow Chemical) was used for the interpenetrating system. $TiCl_3AA$ (AA: activated aluminum metal) and $AlEt_2Cl$ (25% in toluene) were used without treatment. Ferrous chloride tetrahydrate and ferric chloride anhydrous (Merck, Republic of Korea) were used as the precursors of iron oxide nanoparticles. Oleic acid (purchased from Merck, Republic of Korea) was formed to the hydrophobic functionalization agent for iron

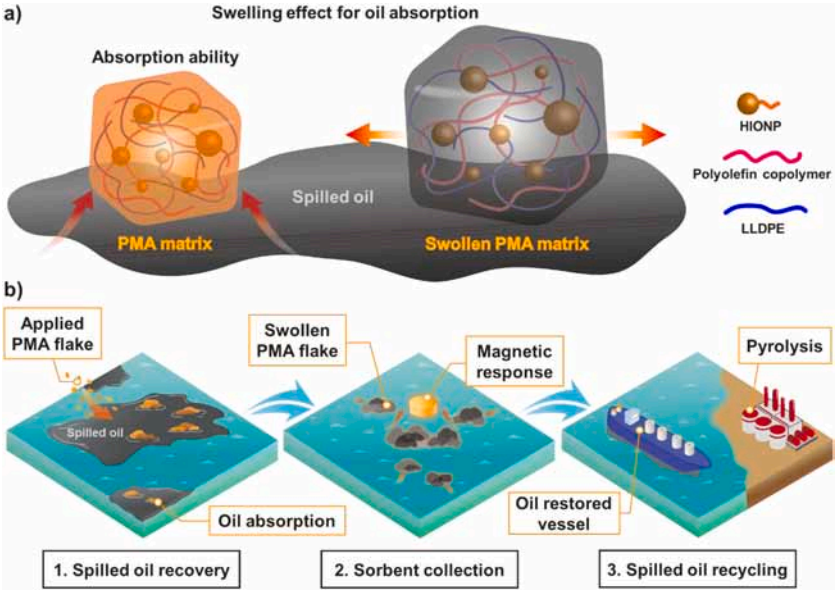

Fig. 1. Schematic illustration of the PMA matrix and oil spill remediation process. (a) Schematic showing the microscopic-scale PMA matrix and swollen PMA matrix. Spilled oil absorption ability of PMA is dominated by swelling effect. (b) Scheme for continuous process of oil spill cleanup as follow: 1. The broad oil spill can be recovered by PMA flakes sprayed over the pollutant region. 2. The oil-soaked PMA flakes are isolated in the aqueous system, then magnet can lead to fast collect for the oil-soaked PMA flakes. 3. The oil-soaked PMA flakes is mainly composed of hydrocarbons which can be directly used as a new energy via a pyrolysis process.

oxide nanoparticles (IONP). The NH_4OH (25 wt% in water, (Merck, Republic of Korea)) was also used as a precipitating agent. Various oils such as diesel, gasoline, and *Arabian* light (AL) crude oil were kindly provided by the Korea Coast Guard. And other organic solvents (n-hexane, toluene, and chloroform) purchased from Merck.

2.2. Preparation of samples

2.2.1. Preparation of polyolefin-based absorbent (PA)

To synthesize the polyolefin copolymer, 1-decene (10 mL) and DVB (0.2 mL) were respectively mixed in a good solvent (i.e., toluene) under nitrogen atmosphere. While agitating the mixtures, the *Ziegler-Natta* catalyst prepared by mixing of $TiCl_3AA$ (0.101 g, 0.0006 mol) and 1 mL of $AlCl_2Et$ (25 wt% in toluene) was added to the solution to initiate the copolymerization reaction under argon purging condition. For the termination, we added the dilute HCl (20% in methanol) and the precipitated 1-decene/DVB copolymer was isolated and rinsed three times with methanol before drying in a vacuum oven at 75 °C overnight. The as-prepared polyolefin copolymer (dissolved in toluene solvent at 100 °C for 2 h) was then interconnected structure mixed with a 1:1 wt ratio of POE (dissolved in toluene solvent at 100 °C for 15 min). Therefore, two dissolved solutions were mixed to make a homogeneous solution at 100 °C for 2 h. The solution was cast onto a pan tray (30 cm × 50 cm × cm) and followed the evaporation step for curing in the oven at 150 °C for 15 min which leads to remain the polyolefin-based absorbent film.

2.2.2. Preparation of hydrophobic functionalized iron oxide nanoparticle (HIONP)

Magnetic nanomaterial (HIONP) was synthesized by co-precipitation process method by precursors (ferrous chloride (1.5 g, 0.012 mol) and ferric chloride (3.0 g, 0.018 mol)). And the precursors were dissolved in water under a nitrogen purging system at an increased temperature from 20 °C to 90 °C. And 10 mL of 25 wt% base agent of NH_4OH (drop by drop 3.33 mL/h) and oleic acid (1.0%, v/v) were supplied to the precursors. IONP could be prepared without supplying oleic acid. Afterward, it could be directly observed that the solution color changed rapidly from dark brown to black. The precipitated HIONP was rinsed with ethanol and DI-water three times. Then, HIONP was remained by drying for 24 h at 80 °C under the vacuum oven.

2.2.3. Preparation of polyolefin-based magnetic absorbent (PMA)

For fabricating the PMA composite, as-prepared HIONP solution (0.1 v/v% for polyolefin solution with dispersed in toluene) was homogeneously mixed in polyolefin dissolution (1:1 wt ratio of polyolefin copolymer and POE) via a solution blending method at 100 °C. Thereafter, a homogeneous blending solution was cast onto a pan tray (30 cm × 50 cm × cm) and followed the evaporation step for curing in the oven at 150 °C for 15 min. Then we could make the PMA film.

2.3. Characterization

To investigate the nanoparticles (IONP and HIONP) morphologies, high resolution-transmission electron microscopy (HR-TEM, JEM-2010) was selected. Field-emission Electron Scanning Microscope (FE-SEM, SUPRA40VP) was also selected to observe absorbents (PA and PMA) morphologies. Attenuated total reflection-*Fourier* transform infrared (ATR-FTIR, Frontier) spectroscopy could observe the functional groups of IONP, HIONP, PA, and PMA range from 500 to 4000 cm^{-1}. 600 MHz Nuclear Magnetic Resonance Spectrometer (600 MHz NMR, JNM-ECZ600R) was also chosen for demonstrating the copolymerized and cross-linked structure of PA. The hydrocarbon component of the original AL crude oil and AL crude oil-soaked PMA0.7 was identified using a High-Resolution Mass Spectrometer (Pegasus GC-HRT). Bomb calorimeter (6400EF) was performed to confirm the using oil fuels compared with several oils and oil-soaked PMA0.7. Multi-Purpose High Performance X-ray Diffractometer (XRD, X′PERT-PRO Powder) could observe the crystallinity of absorbents (PA and PMA). For rheological measurement, viscosities of blending solutions (absorbents dissolved in toluene at ambient temperature for 2 h, 10%, v/v) were performed as shear rate swept from 0.01 to 100 s^{-1} on a rheometer (LVDV-III) using 50 mm Steel parallel plate geometry and 10 cm gap at 25 °C. Differential Scanning Calorimetry (DSC, DSC Q20) also could check the relative comparison of hydrophobic interactions by investigating glass transition temperature. Magnetic property measurement system (MPMS SQUID VSM, MPMS3 Evercool) was used to study the magnetic properties of PMA depends on the amounts of HIONPs.

2.4. Evaluation of oil absorption performance and absorbents crystallinity

DI-water (150 mL) and all oil types (20 mL) were placed into a beaker to simulate the oil spill. Then all oil absorbents (PA and PMAs) were added to the oil spill site under the equal conditions at 25 °C. After the specific time, oil-laden absorbents were observed and absorption capacity (Q_s) was identified by Eq. (1), and the crystallinity (x_c) of PMAs different with HIONP embedding concentration was calculated by Eq. (2):

$$Q_s = (W_s + \quad W_i)/W_i \tag{1}$$

Where W_i is the initial weight of the absorbent sample and W_s is the total weight after a specific time.

$$x_c(\%) = \text{Area of crystalline } peaks/\text{Area all } peaks \times 100 \tag{2}$$

3. Results and discussion

3.1. Preparation of the PMA

The fabrication process for polyolefin-based magnetic absorbent (PMA) followed the previous polymerization pathway of polyolefin oil sorbent (Nam et al., 2018a, 2018b, 2018c). To enhance the oil removal performance, the fabrication process began with dissolving the amorphous elastomer and linear-low density polymer. The olefin copolymer was synthesized with 1-decene and divinylbenzene (DVB) which could lead to the thermally cross-linking structure (between styrene moieties) (Khuong et al., 2005; Kothe and Fischer, 2001). Evidence of the cross-linking was confirmed by proton nuclear magnetic resonance (^1H NMR) spectroscopy. Also, with cross-sectional scanning electron microscopy (SEM) analysis offered the micron scale pores at the polyolefin-based absorbent (PA) surface, confirming the formation of interpenetrated network (IPN) between polyolefin chains through polymerization and polyolefin elastomer (POE) (Fig. S1a-c).

To introduce the magnetic property in the polyolefin sorbent, the as-prepared IPN-structure polyolefin solution was blended with hydrophobic functionalized iron oxide nanoparticle (HIONP) (Figs. 2a and S2). The iron oxide nanoparticle (Fe_3O_4 called IONP) was selected due to its superparamagnetic behavior, high saturation magnetization, and non-toxicity (Kumar et al., 2010; Petcharoen and Sirivat, 2012). For preparing uniformly dispersed Fe_3O_4 nanoparticles in polyolefin solution, the hydrophilic Fe_3O_4 nanoparticles coated with the oleic acid. The oleic acid was chosen as the hydrophobic functionalization agent, due to the hydrocarbon chain of octadecene in the structure as well as the waterproof properties (Liu et al., 2006). The synthesized HIONP can be well dispersed in organic solvent, suggesting it can be homogeneously blended with polyolefin dissolution under 100 °C. A stable dispersion state of HIONP in the polyolefin solution can lead to uniformly dispersed nanoparticle matrix for the PMA film. The as-prepared PMA film showed an optical difference with PA film as a milky-brown color and also good mechanical property (Figs. 2b and S1d-e).

For observing chemical composition of nanoparticle, we performed attenuated total reflection-*Fourier* transform infrared (ATR-FTIR) spectroscopy test. Compared to bare-IONP, the HIONP showed the peak at

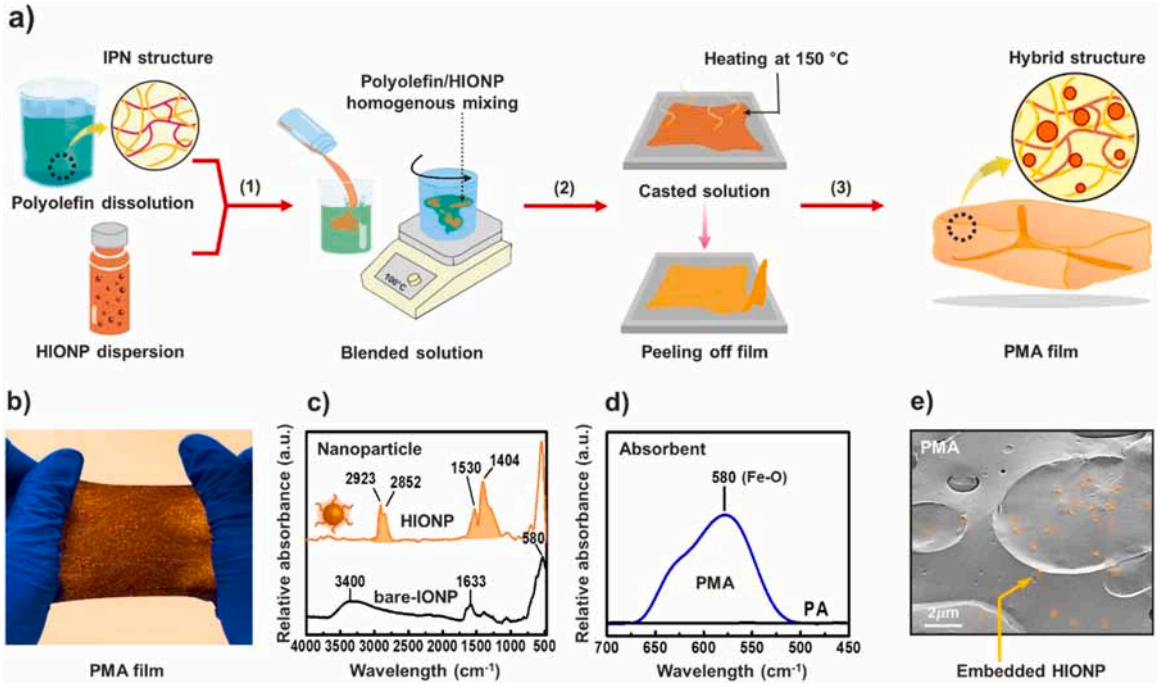

Fig. 2. Schematic illustration of the fabrication process of PMA. (a) 1. The as-prepared polyolefin dissolution is prepared as IPN structure between polyolefin copolymer (D/DVB, red line) and POE (yellow line). Then, the polyolefin solution is homogeneously mixed with HIONP dispersion via a solution blending method. 2. The mixed solution is cast on to a pan tray, and through the solvent evaporation step at 150 °C. 3. The PMA film is remained, which has hybrid structure interacted with HIONP (orange dot) and polyolefin chains. (b) An optical image of a PMA film. (c) ATR-FTIR spectra of bare-IONP (black line) and HIONP (orange line) for distinguishing functionalization of nanomaterial. (d) Magnified ATR-FTIR spectra of PA (black line) and PMA (blue line) for distinguishing HIONP embedding matrix. (e) Cross-sectional SEM image of PMA morphology with embedding nanoparticles (orange circle indicates the HIONP).

580 cm^{-1} (Fe-O group) of iron oxide as well as the new peaks at 1404, 1530 (asymmetric and symmetric stretching of COO^-), 2852, and 2923 cm^{-1} (asymmetric and symmetric of CH_2) for oleic acid (Fig. 2c). The peaks at 3400 and 1633 cm^{-1} (stretching of OH) disappeared, indicating that the carboxyl group of oleic acid was induced after the functionalization process on the spherical surface of nanoparticle. To further demonstrate the functionalization process, the high resolution-transmission electron microscopy (HR-TEM) also revealed the morphological difference of core-sheathe structure between bare-IONP and HIONP (Fig. S3). The as-prepared HIONP was dispersed in toluene to form a colloidal state, then the HIONP dispersion was added to the polyolefin solution with vigorous stirring. And the mixed solution was

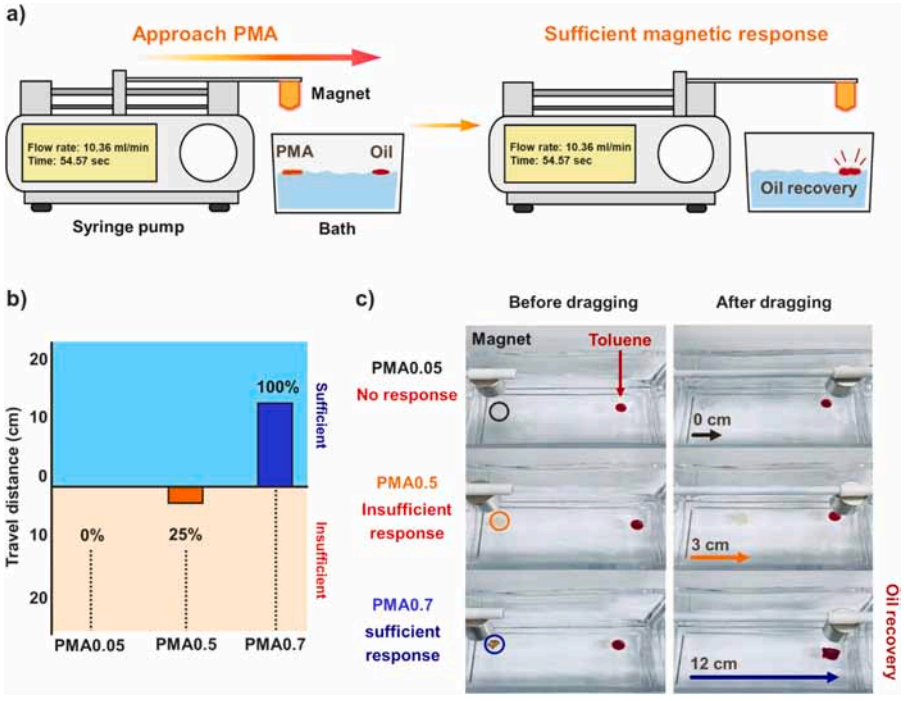

Fig. 3. Schematic of a magnetic dragging system for observing travel distance of PMAs for several HIONP concentrations (0.05, 0.5, and 0.7 wt%). (a) The magnetic dragging system is constructed by syringe pump with constant dragging speed of magnet (flow rate is 10.36 mm/min and running track distance is 12 cm which takes 54.57 s to reach the spilled oil spot of end-line) and constant height from PMA (5.6 cm). (b) The travel distance of the PMAs with several HIONP concentrations (0.05 wt% of PMA0.05, 0.5 wt% of PMA0.5, and 0.7 wt% of PMA0.7) adapted in magnetic dragging system. (c) Digital photographs of magnetic dragging with several HIONP concentrations (0.05, 0.5, and 0.7 wt%) via home-made magnetic dragging system.

evaporation at 150 °C with the same fabrication procedure as PA. The ATR-FTIR spectroscopy demonstrated the hybrid structure of PMA, as indicated by the show up of iron oxide peak at 580 cm^{-1} for Fe-O group (Fig. 2d). Therefore, PMA can effectively react with external magnetic force and showed para-magnetism (Fig. S4). The SEM image shows that HIONP was uniformly dispersed in the PMA matrix, representing that HIONP has high affinity with polyolefin chain (Fig. 2e).

3.2. Magnetic response of the PMA

Due to the addition of HIONP to the polyolefin matrix, the PMA can be dragged by magnetic force on water surface. Low HIONP concentration cannot induce the magnetic property to PMA, indicating that optimized minimal concentration of HIONP is needed for efficient magnetic collection of PMA. Then, we fabricated a magnetic dragging system for PMA, which has a constant dragging speed and a constant height, for identifying the optimized HIONP concentration (Fig. 3a). Under magnetic field, the PMA can be fixed on the water surface and efficiently approach to the oil spilled spot of end-line as soon as magnetic dragging system starts up. Different HIONP concentration for PMAs (PMA0.05, PMA0.5, and PMA0.7) showed different travel distance at the aqueous state (Fig. 3b and Movie S1). Compared to the PMA0.05 showing only 0 cm and PMA0.5 showing only 3 cm, PMA0.7 only could touch the oil spilled spot (dyed with Oil red O), which indicated that less than 0.7 wt% of PMAs (PMA0.05 and PMA0.5) had insufficient magnetic reaction (Fig. 3c). Thus, more than 0.7 wt% of HIONP concentration for PMA can show magnetic controlled properties efficiently.

Supplementary material related to this article can be found online at doi:10.1016/j.jhazmat.2021.126485.

To apply in broad oil spill area and realize fast oil removal, the PMA0.7 film is adapted into the flake type with facile grinding method of easy sample handling. Owing to its good elasticity, the PMA0.7 can be transformed into a tiny flake morphology, which provide the enhanced oil removal speed due to macroscopically increased specific surface area (Fig. S5). Furthermore, the obtained flake type sorbent can cover the widespread oil spilled sites at the open sea. However, such small-sized flake can be dispersed widely on the water due to marine condition, they are possible to create isolated regions individually. Although, some flakes voluntarily close due to the marine wave and their affinities, massive amounts of flakes are remained on the water surface. Thus, employing external magnetic force can harvest the isolated flakes at once (Fig. 4a). To demonstrate the sorbent separation via a magnet, the AL crude oil were spilled in the aqueous (Fig. 4b**).** The PMA0.7 flakes could be applied combating for each isolated oil spots like dispersants applied, the applied PMA0.7 flakes fully absorbed spilled oil and formed adducted with connected swollen flakes after 30 min Finally, the AL crude oil soaked-PMA0.7 flakes was fast collected when the magnet approaching. We also observed the same process combating for AL crude oil (mixture oil), toluene (pure solvent), and gasoline (refined oil) (Fig. S6 and Movie S2). This magnetic collection process ensured short time oil removal of the flake type PMA0.7 regardless of oil types, and magnetic collection is an efficient method for isolated flakes in the broad area.

Supplementary material related to this article can be found online at doi:10.1016/j.jhazmat.2021.126485.

Although, the numerous sprayable magnetic oil sorbents have been reported such as nanomaterial and biomass-derived sorbents (Chen et al., 2018; Dai et al., 2018; Gan et al., 2016; Navarathna et al., 2020; Yang et al., 2017; Zhu et al., 2010). These sprayable sorbents could not show effective oil removal performance which is mainly due to intrinsic low affinity with oil and low specific surface area. Compare with other

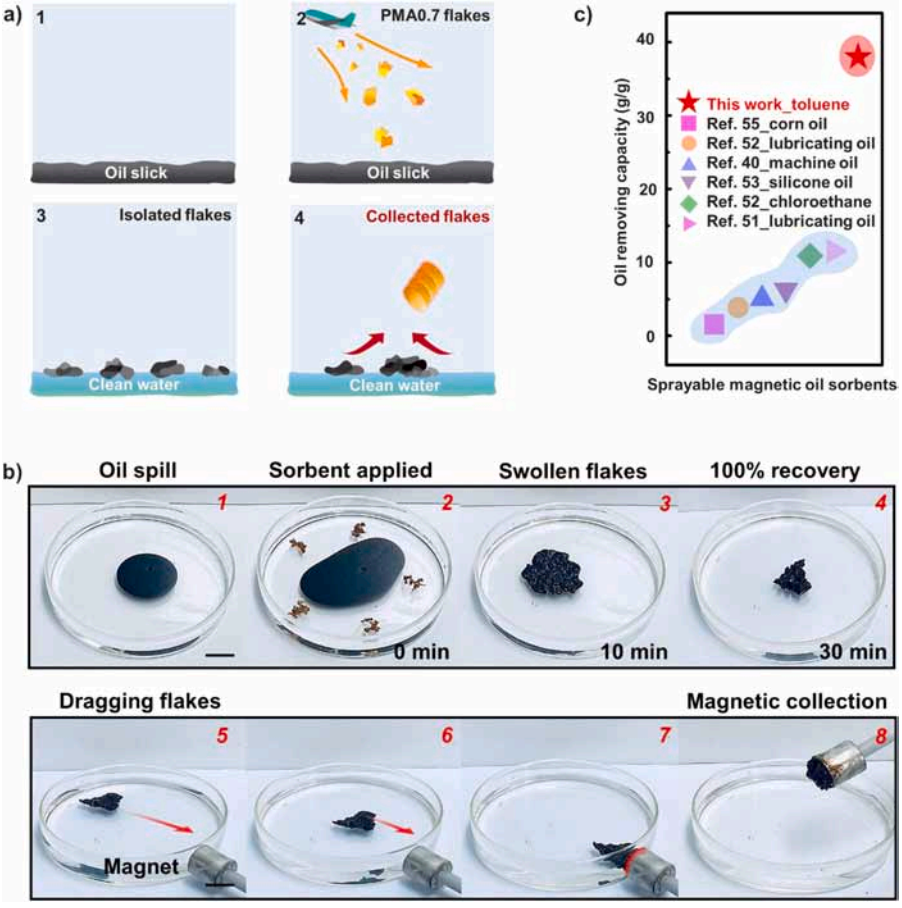

Fig. 4. (a) Schematic illustration of magnetic collection process for PMA0.7 flake. (b) Photographs of the magnetic collection process for oil-soaked PMA flakes 1. The AL crude oil spill regions spread on the water. 2. The PMA0.7 flakes (0.05 g) were placed onto spilled oil region. 3. After 10 min, PMA0.7 flakes absorbed spilled AL crude oil and rapidly swollen its own volume. 4. After 30 min, AL crude oil-soaked PMA0.7 flakes shown swollen and formed adducts with viscously connected state. 5–8. The magnet could pull on adduct of AL crude oil-soaked PMA0.7 flakes at once, and easily detached from the water surface. (c) Comparison of the oil removal performance of flake type PMA0.7 and among reported sprayable magnetic oil sorbents.

studies, PMA0.7 flake showed superior oil removal performance (Fig. 4c). The high oil removal value is closely related with the intrinsic oleophilic characteristic inherited from polyolefin chemical structure. From these processes, we propose that transforming shape of oil sorbent to the flake type is practical for applying in broad oil spill sites. Moreover, magnetic nanoparticles containing flake type PMA0.7 implies significantly promising applications for big oil spill.

3.3. Oil recovery performance of the PMA

In contrast to the capillary effect of common oil sorbents (Cui et al., 2020; Song et al., 2020; Wu et al., 2013, 2016, 2021), the PMA mainly relies on the swelling characteristic with a hydrocarbon polymeric matrix allowing for highly oil absorption property without oil leakage (Fig. S7). The prefabricated polyolefin-based oil sorbents with various colors, white, milky-brown, and dark brown color of different color saturation, are depended on the concentration of HIONP as shown in Fig. 5a. Similar to hydrogel-formed materials, the PMA and can selectively absorb several oil liquids in an aqueous system. Therefore, two outstanding regions of curve were observed in the swelling ratio (R_s) to time (Fig. 5b–d). Increasing R_s region with an oil absorption time around 30 min indicates that initially oil soaking to internal space of interconnected polyolefin matrix. Then, the R_s shows plateau region after 30 min corresponds to the equilibrated swelling state (E_s) of PMAs, which can reach at 6 h regardless of oil type. Concurrently, we also observed the oil absorption trend with toluene, gasoline, and AL crude oil. This absorption trend represents that toluene can diffuse into the amorphous matrix of PMA due to its good solvent for polyolefin. Conversely, more complex oil such as gasoline and AL crude oil showed lower absorptions to PMA, indicating that they have relative more portion of poor solvent which leads to difficulty of oil diffusion in the polyolefin matrix (Nam et al., 2016a, 2016b). Furthermore, the overall swelling ratios declined conspicuously with increasing HIONP concentration of PMAs (PMA0.7, PMA1, PMA5, and PMA10 indicates relative added concentration of HIONP respectively). This declined tendency with increasing HIONP concentration also indicates that the embedding of HIONP results in increasing nanoparticle-polymer interactions (Fig. 5e).

The HIONP behaves as a physical crosslinking agent in the PMA matrix. The physical cross-linking can be formed by alkyl chain association between functionalization agent of HIONP and polyolefin chain. Thus, the nanomaterial is act as a physical cross-linking point for sorbent matrix (Chen et al., 2019; Chern, 2006), indicating that cross-linking point of HIONP forms more densely structure of PMA. X-Ray Diffraction (XRD) analysis was employed for observing cross-linking point content for HIONP concentration (Fig. 6a). For the HIONP, the peaks of 30.30°, 35.65°, 43.24°, 50.65°, 57.38°, and 62.89° reflect the magnetite crystal with a cubic spinel structure. The distinct peak of PA indicates remarkably broad peak of 20.04° means amorphous carbon. Therefore, the more HIONP concentration was added to the sorbent matrix, distinct peak of magnetite was increasingly stood out for PMA. Therefore, from XRD spectra, we could calculate the crystallinity (x_c) of PMAs, which increased with the addition of HIONP, indicating an increase in physical cross-linking point (Fig. 6b).

Moreover, rheological analysis is also substantial information for physical cross-linking of PMA. Thus, measuring the solution viscosity as a function of shear rate can provide physical cross-linking degree, indicating the hydrophobic interaction degree (Fig. 6c). Therefore, the re-dissolved PMA solution (in good solvent) was increased viscosity with adding HIONP. This is mainly attributed to the increasing hydrophobic interaction between octadecene chain of HIONP and polyolefin chain. Furthermore, all PMA dissolutions was also shown a decreasing viscosity with increasing shear rates regardless of HIONP concentration. This phenomenon can be interpreted as a non-Newtonian and shear-thinning fluids. The massive amount of hydrophobic interaction between alkyl chains is broken due to the increasing shear rates.

To define the hydrophobic interaction obviously, thermal analysis of differential scanning calorimetry (DSC) was chosen for the microscopic thermal motion of PMAs (Fig. 6d). The polymeric oleic acid can be applied as a plasticizer which is located at the free-volume space of polyolefin chains (Cerrada et al., 2000; Chern, 2006; Scott et al., 1994). Adding plasticizer can occur the weaker interaction between polymer chains, the higher flexibility of polymer chains, indicating that longer range segmental motions to occur at lower temperature (Immergut and Mark, 1965; Nambiar and Blum, 2008). Therefore, we can interpret, decreasing T_g with increasing HIONP concentration in the polyolefin matrix, physically weak interaction of hydrophobic association.

The polymer chains are closer to each other, which is mainly attributed to hydrophobic interaction between HIONP and polyolefins, occurring densely structures hindered swelling performance (Mahanta et al., 2013). Thus, the higher the HIONP concentration in the PMA, the less swelling of oil absorbent. In consequence, we can conclude that

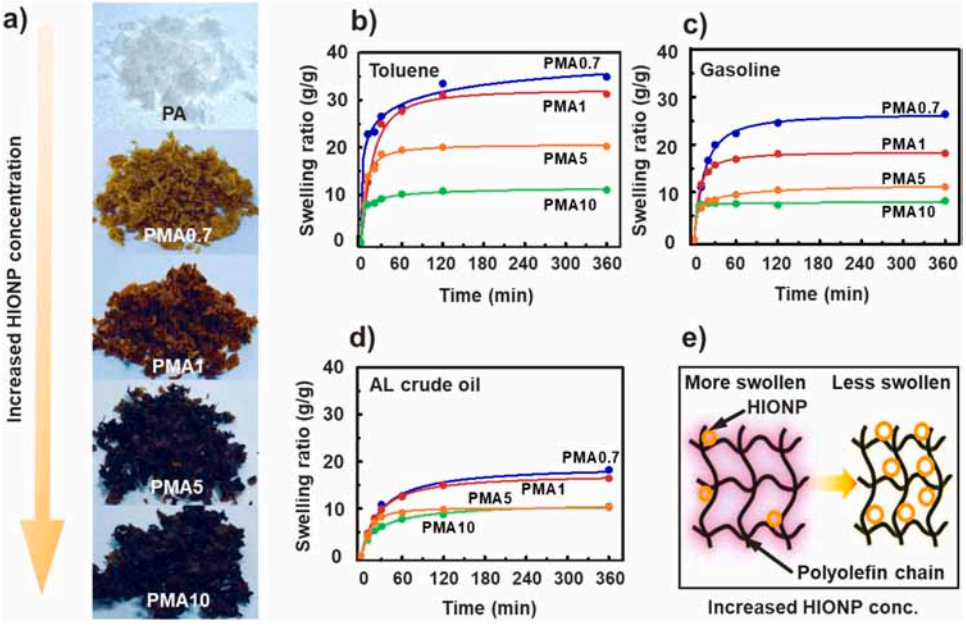

Fig. 5. Absorption performance according to several oils with PMAs. (a) Optical photographs of PA and various PMAs according to the HIONP concentration. (b–d) Absorption profiles for different HIONP concentration of PMAs (0.7, 1, 5, and 10 wt% of HIONP) for toluene (left), gasoline (middle), and AL crude oil (right). These continuous lines guide the eyes denoting the trend of the experimental results. (e) Schematic illustration of swelling performance of PMA for HIONP concentration. The higher concentration of HIONP leading to increased physically interaction with polyolefin matrix, reflecting less swelling.

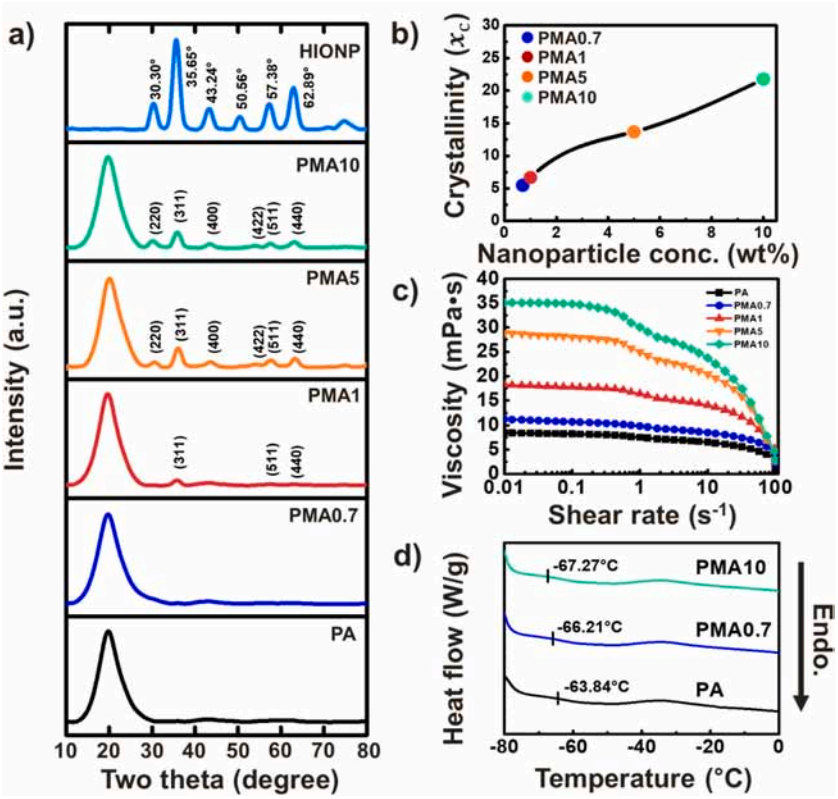

Fig. 6. The characterizations of the physical cross-linking for crystallinity of PMAs. (a) XRD analysis for characterization of HIONP, PA, and PMA with different concentration of HIONP (PMA0.7, PMA1 PMA5, and PMA10). (b) Crystallinity of PA and PMA with different concentrations of HIONP (PMA0.7, PMA1, PMA5, and PMA10). (c) Shear viscosity for PA and PMA with different concentrations of HIONP dissolved in good solvent (dissolving under 2 h). (d) DSC analysis for measurement T_g for PA, PMA0.7 and PMA10.

0.7 wt% of HIONP for PMA is optimized concentration for excellent magnetic dragging without affect the swelling performance.

Of particular interest is that PMA matrix showed highly dispersed HIONP structure. Dispersion of nanomaterials is one of the major importance for polymeric nanocomposite matrix (Deng et al., 2016; Feng et al., 2012). The nanocomposite with good dispersion of nanomaterials is necessary for the development of high-performance materials because of strong interparticle interactions and weak polymer-nanomaterial interfacial interactions. Especially, the swelling kinetic parameter, which dominates oil absorption performance, is strongly influenced by nanomaterial chemical property and concentration (Panic et al., 2015). Therefore, to efficiently disperse nanoparticles in the nanocomposite matrix of sorbent, a hydrophobic functionalized agent of IONP was chosen. The hydrophobic agent (i.e., octadecene of oleic acid) has long hydrocarbon chains, which can arouse high affinity in the polyolefin matrix. Because of its good affinity, between the polyolefin matrix and hydrophobic functionalization agent (Liu et al., 2011; Park et al., 2006; Wu et al., 2014), they can lead to physical interaction (alkyl chain association). To observe the dispersed matrix of PMA, energy dispersive spectroscopy (EDS) mapping was chosen, results that the HIONP can be dispersed effectively due to good affinity with polyolefin (Fig. S8). Thus, the PMA can perform the dual characteristics of swelling ability and reacting with magnetic field in the aqueous system due to its highly dispersed HIONP.

The optimized PMA0.7 was shown good equilibrated swelling ratio for several oils, demonstrating that the optimized PMA0.7 significantly showed no difference of equilibrated swelling values compared to the PA (i.e., no embedding HIONP) (Fig. 7a). However, other PMAs (PMA1, PMA5, and PMA10) also showed a declined tendency as equilibrated swelling values, indicating that the optimized PMA0.7 was superior sample for oil removal (Fig. 7b-d). Then, we optically observed the swelling phenomenon of PMA0.7 film (Fig. 7e). After 6 h, the obtained AL crude oil-soaked PMA0.7 film reached almost 5.2 times for the film length. In the height distance aspect, the PMA0.7 film, which is folded several films for visually checking, also showed swollen difference from 0.4 to 0.6 mm. These results repeatedly demonstrate that optimized HIONP concentration of PMA can efficiently show the swollen ability for oil removal performance.

3.4. Recycling after oil recovery

Since the polyolefin itself has valuable oil fuel energy (Panda et al., 2010), the oil-soaked PMA0.7 flake can be directly converted into refined oils via a pyrolysis process and remained carbonized mixture. The remained carbonized compounds, which are contained carbonized residue, also are separated by magnetic recovery process then reused. The PMA0.7 flakes could absorb AL crude oil 14.92 times of its own weight as identify magnetic nanoparticle recovery process (Fig. 8a). Crude oil was selected for complex oil. During the pyrolysis process at 600 °C, AL crude oil-soaked PMA0.7 flakes processed through carbonization. Upon heating AL crude oil-soaked PMA0.7 flake, almost low boiling point substances can deform to the refined oil fuels such as gasoline, naphtha, diesel, etc. via a distillation and extraction process in the petroleum industries. In the heating furnace, carbonized compounds were left with carbon residue and magnetic nanoparticles. The IONP could be separated by a magnet and shown 1.86×10^{-3} g of magnetic nanoparticle recovered. This less content of magnetic nanoparticle may indicate the loss of the nanomaterials during fabrication or separation process. Furthermore, pyrolyzed magnetic nanoparticles peeled off oleic acid coating could be recycled several times for sorbent fabrication with re-functionalization for oleic acid (Fig. S9) (Patil et al., 2014).

More interestingly, all two spectra of gas chromatography-mass spectroscopy (GC-MS) analysis shows that the original AL crude oil and the AL crude oil-soaked PMA0.7 flake were almost indistinguishably equal peak line (Fig. 8b). The AL crude oil-soaked PMA0.7 flake decomposed into hydrocarbon components (C_8H_{18} to $C_{20}H_{42}$) for retention time from 0 s to 4000 s, suggesting that oil-soaked PMA0.7 flake can be completely recycled to oil fuels. Furthermore, the portion of hydrocarbon component was also measured from the relative peak area of GC-MS analysis (Fig. 8c). The relative portion of hydrocarbon

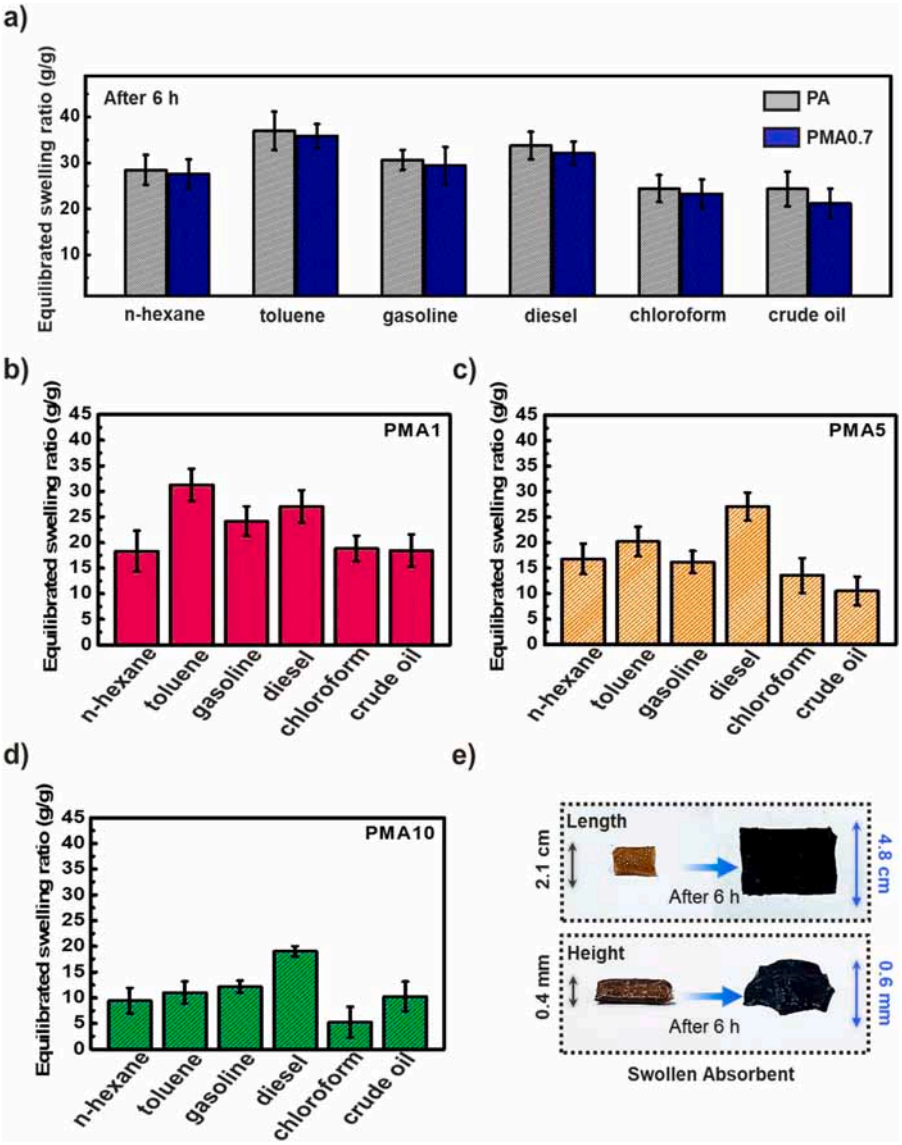

Fig. 7. (a–d) Comparison equilibrated swelling kinetics of PA and PMAs (PMA0.7, PMA1, PMA5, and PMA10) with several oils (n-hexane, toluene, gasoline, diesel, chloroform, and crude oil) after 6 h. (e) Photographs to observe the swelling phenomenon of PMA0.7 film for the length (a single layer) and height (several folded layers to identify the swollen well) after 6 h.

component for the AL crude oil-soaked PMA0.7 flake increased from decane ($C_{10}H_{22}$) to eicosane ($C_{20}H_{42}$), indicating that AL crude oil-soaked PMA0.7 flake comprised with hydrocarbons with longer chains. The AL crude oil-soaked PMA0.7 flake has polyolefin mixture which is mainly composed of 1-decene and POE. This polyolefin components lead to its increased hydrocarbon components from $C_{10}H_{22}$ to $C_{20}H_{42}$.

To further demonstrate oil fuel value, combustion process of bomb calorie meter was characterized the heating calorific values of several original oils and oil-soaked PMA0.7 flake. As shown in Fig. 8d, the heating calorific values of oil-soaked PMA0.7 flake was similar to the several original oils. Each heating values of oil-soaked PMA0.7 flake (i.e., toluene 34.82, n-hexane 28.66, diesel 31.07, gasoline 37.48, chloroform 31.37, and AL crude oil 32.25 MJ/kg) were slightly higher than the several original oils (i.e., toluene 31.05, n-hexane 27.52, diesel 29.90, gasoline 35.59, chloroform 30.21, and AL crude oil 30.86 MJ/kg), suggesting that polyolefin sorbent effects to the heating calorific values and shown excellent oil fuel value with regard to polyolefin, which is commonly derived from petroleum industry. Thus, oil-soaked PMA0.7 flake demonstrates one of the potential oil fuels among reported oil sorbents. In the meantime, abundantly reported oil sorbents have shown the continuous oil reusability process with oil sorption-desorption to recycle the spilled oil (Kim et al., 2015; Si et al., 2015; Song et al., 2020; Wu et al., 2021). They mainly focused on the mechanical properties of sorbents for repeatedly compressive strain, suggesting that process is dominated by outer power source. The hydrocarbon structure of PMA0.7 can offer sustainably oil recycling process for environment.

4. Conclusion

In conclusion, we prepared polyolefin-based magnetic absorbent (PMA) by introducing hydrophobic functionalized iron oxide nanoparticle (HIONP). The adding HIONP to the polyolefin matrix shows highly dispersed structures, then improves collection process of the sorbents after oil spill recovery. Moreover, its enhanced chemical structure, blended with low-crosslinked polymer (LCP) and polyolefin elastomer (POE), can absorb the liquid oils with swelling ability. PMA shows with 37 g/g of organic liquid and 24 g/g of crude oil in 6 h. Compared with developed sorbents, the PMA can transform into the tiny

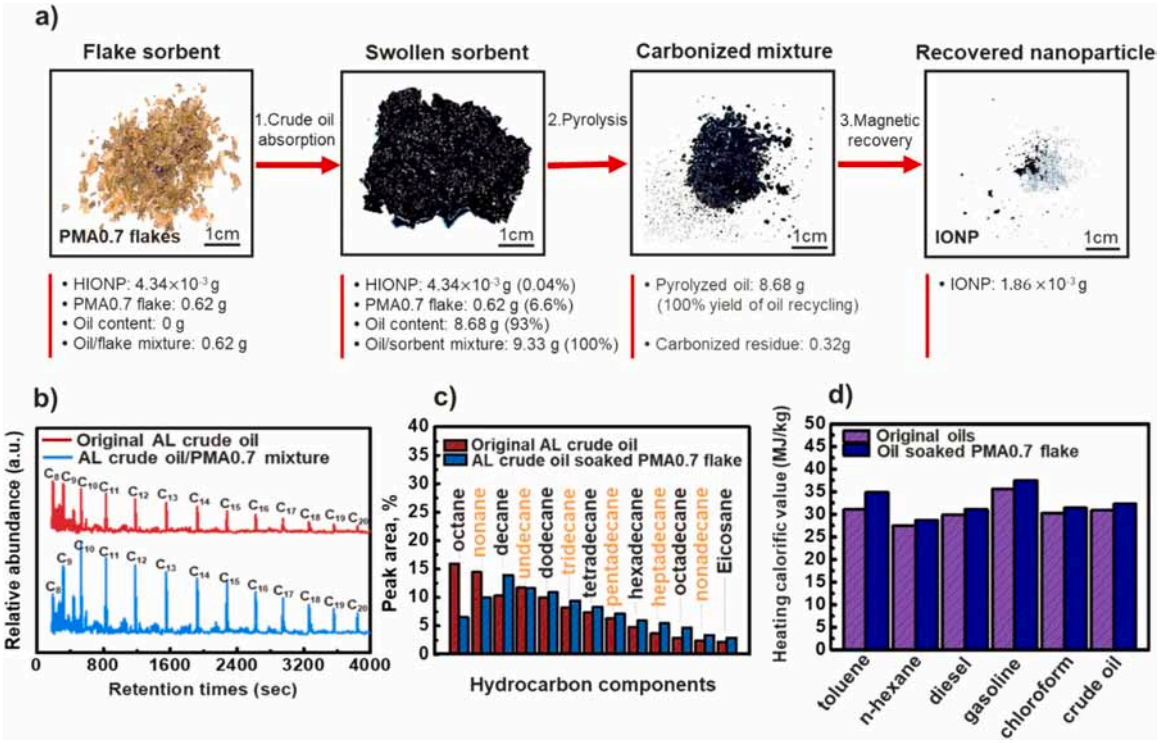

Fig. 8. Recycling characterization of oil-soaked PMA0.7 flake. (a) Optical photographs showing carbonized compounds separation after pyrolysis process: 1. PMA0.7 flakes (0.62 g) soak the 14.92 times (8.68 g) of AL crude oil. 2. Swollen PMA0.7 flakes are converted into carbonized compounds through the pyrolysis process at 600 °C, which is contained 0.32 g of carbonized residue. 3. IONP (0.00186 g) can be separated by magnetic recovery process. (b) GC-mass spectra of original AL crude oil (red line) and AL crude oil-soaked PMA0.7 flake (1:1 wt ratio, blue line) for retention time 0–4000 s. (c) Comparison of the relative amount of hydrocarbon components with original AL crude oil (red box) and AL crude oil-soaked PMA0.7 flake (blue box) derived from peak area of GC-mass spectra for retention time 0–4000 s. (d) Bomb calorimeter heating values for several original oils (purple box) and oil-soaked PMA0.7 flake (blue box).

architectures like flakes owing to thermoplastic deformation of polyolefin characterization. Thus, they can cover the broad organic pollutant regions by spraying to the broad marine. An interesting polymer-nanomaterial hybridized PMA also used for oil fuels after oil recovery. The oil-soaked PMA, which is mainly comprised of hydrocarbons, can be directly converted into oils via pyrolysis process under 600 °C. The developed PMA can propose a new technology of oil sorbents fields and environmentally solution for oil spills, reducing unintentional pollutions.

CRediT authorship contribution statement

Hyeongoo Kim: Formal analysis, Investigation, Methodology, Writing - original draft. **Gang Zhang**: Synthesis, Writing - review & editing. **Min Wu**: Resources, Data curation. **Jinshan Guo**: Writing - review & editing, Supervision. **Changwoo Nam**: Conceptualization, Project administration, Funding acquisition.

Declaration of Competing Interest

The author declare that they have no known competing financial interests or personal relationship that could have appeared to influence the work reported in this paper.

Acknowledgments

This work was supported by the National Research Foundation of Korea (NRF) grant funded by the Korea government (MSIT) (No. F2020R1F1A1052087).

Appendix A. Supporting information

Supplementary data associated with this article can be found in the online version at doi:10.1016/j.jhazmat.2021.126485.

References

Al Absi, A.A., Aitani, A.M., Al Khattaf, S.S., 2020. Thermal and catalytic cracking of whole crude oils at high severity. J. Anal. Appl. Pyrolysis 145, 104705.
Almeda, R., Cosgrove, S., Buskey, E.J., 2018. Oil spills and dispersants can cause the initiation of potentially harmful dinoflagellate blooms ("Red Tides"). Environ. Sci. Technol. 52, 5718–5724.
Asadpour, R., Sapari, N., Tuan, Z., Jusoh, H., Riahi, A., Uka, O., 2013. Application of sorbent materials in oil spill management: a review. Casp. J. Appl. Sci. Res 2, 46–58.
Cerrada, M.L., Benavente, R., PEREZ, E., PERENA, J.M., 2000. The effect of residual acetate groups on the structure and properties of vinyl alcohol-ethylene copolymers. J. Polym. Sci. Part B Polym. Phys. 38, 573–583.
Chen, H.-J., Hang, T., Yang, C., Liu, G., Lin, D., Wu, J., Pan, S., Yang, B., Tao, J., Xie, X., 2018. Anomalous dispersion of magnetic spiky particles for enhanced oil emulsions/water separation. Nanoscale 10, 1978–1986.
Chen, J., An, R., Han, L., Wang, X., Zhang, Y., Shi, L., Ran, R., 2019. Tough hydrophobic association hydrogels with self-healing and reforming capabilities achieved by polymeric core-shell nanoparticles. Mater. Sci. Eng. C 99, 460–467.
Chen, Z., An, C., Yin, J., Owens, E., Lee, K., Zhang, K., Tian, X., 2021. Exploring the use of cellulose nanocrystal as surface-washing agent for oiled shoreline cleanup. J. Hazard. Mater. 402, 123464.
Chern, C.S., 2006. Emulsion polymerization mechanisms and kinetics. Prog. Polym. Sci. 31, 443–486.
Chung, T.C.M., 2013. Functional polyolefins for energy applications. Macromolecules 46, 6671–6698.
Cui, Y., Wang, Y., Shao, Z., Mao, A., Gao, W., Bai, H., 2020. Smart sponge for fast liquid absorption and thermal responsive self-squeezing. Adv. Mater. 32, 1908249.
Dai, J., Zhang, R., Ge, W., Xie, A., Chang, Z., Tian, S., Zhou, Z., Yan, Y., 2018. 3D macroscopic superhydrophobic magnetic porous carbon aerogel converted from biorenewable popcorn for selective oil-water separation. Mater. Des. 139, 122–131.
Dave, 2011. Remediation technologies for marine oil spills: a critical review and comparative analysis. Am. J. Environ. Sci. 7, 424–440.

Deng, Z., Jiang, Y., He, L., Zhang, L., 2016. Aggregation–dispersion transition for nanoparticles in semiflexible ring polymer nanocomposite melts. J. Phys. Chem. B 120, 11574–11581.
Feng, Y., Zou, H., Tian, M., Zhang, L., Mi, J., 2012. Relationship between dispersion and conductivity of polymer nanocomposites: a molecular dynamics study. J. Phys. Chem. B 116, 13081–13088.
Fuller, C., Bonner, J.S., 2001, Comparative toxicity of oil, dispersant, and dispersed oil to texas marine species. Int. Oil Spill Conf. Proc. 2001, 1243–1248.
Gan, W., Gao, L., Zhang, W., Li, J., Cai, L., Zhan, X., 2016. Removal of oils from water surface via useful recyclable CoFe 2 O 4 /sawdust composites under magnetic field. Mater. Des. 98, 194–200.
Gao, Y., Liu, W., Zhu, S., 2017. Polyolefin thermoplastics for multiple shape and reversible shape memory. ACS Appl. Mater. Interfaces 9, 4882–4889.
Ge, J., Zhao, H.Y., Zhu, H.W., Huang, J., Shi, L.A., Yu, S.H., 2016. Advanced sorbents for oil-spill cleanup: recent advances and future perspectives. Adv. Mater. 28, 10459–10490.
Graziele da Costa Cunha, G., Pinho, N.C., Alves Silva, I.A., Santos Silva, L., Santana Costa, J.A., da Silva, C.M.P., Romão, L.P.C., 2019. Removal of heavy crude oil from water surfaces using a magnetic inorganic-organic hybrid powder and membrane system. J. Environ. Manag. 247, 9–18.
Gu, J., Fan, H., Li, C., Caro, J., Meng, H., 2019. Robust superhydrophobic/superoleophilic wrinkled microspherical MOF@rGO composites for efficient oil–water separation. Angew. Chem. Int. Ed. 58, 5297–5301.
Gui, X., Li, H., Wang, K., Wei, J., Jia, Y., Li, Z., Fan, L., Cao, A., Zhu, H., Wu, D., 2011. Recyclable carbon nanotube sponges for oil absorption. Acta Mater. 59, 4798–4804.
Gui, X., Wei, J., Wang, K., Cao, A., Zhu, H., Jia, Y., Shu, Q., Wu, D., 2010. Carbon nanotube sponges. Adv. Mater. 22, 617–621.
Gui, X., Zeng, Z., Lin, Z., Gan, Q., Xiang, R., Zhu, Y., Cao, A., Tang, Z., 2013. Magnetic and highly recyclable macroporous carbon nanotubes for spilled oil sorption and separation. ACS Appl. Mater. Interfaces 5, 5845–5850.
Guvendiren, M., Yang, S., Burdick, J.A., 2009. Swelling-induced surface patterns in hydrogels with gradient crosslinking density. Adv. Funct. Mater. 19, 3038–3045.
Immergut, E.H., Mark, H.F., 1965. Plasticization and plasticizer processes. plast. Plast. Process 48, 1–26.
Ivshina, I.B., Kuyukina, M.S., Krivoruchko, A.V., Elkin, A.A., Makarov, S.O., Cunningham, C.J., Peshkur, T.A., Atlas, R.M., Philp, J.C., 2015. Oil spill problems and sustainable response strategies through new technologies. Environ. Sci. Process Impacts 17, 1201–1219.
Kaminsky, W., 1996. New polymers by metallocene catalysis. Macromol. Chem. Phys. 197, 3907–3945.
Karatepe, N., 2003. Adsorption of a non-ionic dispersant on lignite particle surfaces. Energy Convers. Manag. 44, 1275–1284.
Khuong, K.S., Jones, W.H., Pryor, W.A., Houk, K.N., 2005. The mechanism of the self-initiated thermal polymerization of styrene. Theoretical solution of a classic problem. J. Am. Chem. Soc. 127, 1265–1277.
Kim, D.H., Jung, M.C., Cho, S., Kim, S.H., Kim, H., Lee, H.J., Oh, K.H., Moon, M., 2015. UV-responsive nano-sponge for oil absorption and desorption. Sci. Rep. 5, 12908.
Kizil, S., Bulbul Sonmez, H., 2017. Oil loving hydrophobic gels made from glycerol propoxylate: efficient and reusable sorbents for oil spill clean-up. J. Environ. Manag. 196, 330–339.
Kleindienst, S., Paul, J.H., Joye, S.B., 2015. Using dispersants after oil spills: impacts on the composition and activity of microbial communities. Nat. Rev. Microbiol. 13, 388–396.
Kothe, T., Fischer, H., 2001. Formation rate constants of the mayo dimer in the autopolymerization of styrene. J. Polym. Sci. Part A Polym. Chem. 39, 4009–4013.
Kumar, R., Inbaraj, B.S., Chen, B.H., 2010. Surface modification of superparamagnetic iron nanoparticles with calcium salt of poly(γ-glutamic acid) as coating material. Mater. Res. Bull. 45, 1603–1607.
Li, J., Tenjimbayashi, M., Zacharia, N.S., Shiratori, S., 2018. One-step dipping fabrication of Fe_3O_4/PVDF-HFP composite 3D porous sponge for magnetically controllable oil–water separation. ACS Sustain. Chem. Eng. 6, 10706–10713.
Liu, J., Gao, Y., Cao, D., Zhang, L., Guo, Z., 2011. Nanoparticle dispersion and aggregation in polymer nanocomposites: insights from molecular dynamics simulation. Langmuir 27, 7926–7933.
Liu, X., Kaminski, M.D., Guan, Y., Chen, H., Liu, H., Rosengart, A.J., 2006. Preparation and characterization of hydrophobic superparamagnetic magnetite gel. J. Magn. Magn. Mater. 306, 248–253.
Liu, Y., Wang, X., Feng, S., 2019. Nonflammable and magnetic sponge decorated with polydimethylsiloxane brush for multitasking and highly efficient oil–water separation. Adv. Funct. Mater. 29, 1902488.
Mahanta, N., Teow, Y., Valiyaveettil, S., 2013. Viscoelastic hydrogels from poly(vinyl alcohol)–Fe(III) complex. Biomater. Sci. 1, 519–527.
Nam, C., Li, H., Zhang, G., Chung, T.C.M., 2016a. Petrogel: new hydrocarbon (oil) absorbent based on polyolefin polymers. Macromolecules 49, 5427–5437.
Nam, C., Li, H., Zhang, G., Lutz, L.R., Nazari, B., Colby, R.H., Chung, T.C.M., 2018a. Practical oil spill recovery by a combination of polyolefin absorbent and mechanical skimmer. ACS Sustain. Chem. Eng. 6, 12036–12045.
Nam, C., Zhang, G., Chung, T.C.M., 2018b. Polyolefin-based interpenetrating polymer network absorbent for crude oil entrapment and recovery in aqueous system. J. Hazard. Mater. 351, 285–292.
Nam, C., Zimudzi, T.J., Geise, G.M., Hickner, M.A., 2016b. Increased hydrogel swelling induced by absorption of small molecules. ACS Appl. Mater. Interfaces 8, 14263–14270.
Nam, C., Zimudzi, T.J., Wiencek, R.A., Chung, T.C.M., Hickner, M.A., 2018c. Improved ATR-FTIR detection of hydrocarbons in water with semi-crystalline polyolefin coatings on ATR elements. Analyst 143, 5589–5596.
Nambiar, R.R., Blum, F.D., 2008. Segmental dynamics of bulk poly(vinyl acetate)- d 3 by solid-state 2H NMR: effect of small molecule plasticizer. Macromolecules 41, 9837–9845.
Navarathna, C.M., Dewage, B., Keeton, N., Pennisson, C., Henderson, J., Lashley, R., Zhang, B., Hassan, X., Perez, E.B., Mohan, F., Pittman, D., Mlsna, T, C.U., 2020. Biochar adsorbents with enhanced hydrophobicity for oil spill removal. ACS Appl. Mater. Interfaces 12, 9248–9260.
Ono, T., Sugimoto, T., Shinkai, S., Sada, K., 2007. Lipophilic polyelectrolyte gels as super-absorbent polymers for nonpolar organic solvents. Nat. Mater. 6, 429–433.
Panda, A.K., Singh, R.K., Mishra, D.K., 2010. Thermolysis of waste plastics to liquid fuel: a suitable method for plastic waste management and manufacture of value added products—a world prospective. Renew. Sustain. Energy Rev. 14, 233–248.
Panic, V.V., Spasojevic, P.M., Radoman, T.S., Dzunuzovic, E.S., Popovic, I.G., Velickovic, S.J., 2015. Methacrylic acid based polymer networks with a high content of unfunctionalized nanosilica: particle distribution, swelling, and rheological properties. J. Phys. Chem. C 119, 610–622.
Park, M.J., Char, K., Park, J., Hyeon, T., 2006. Effect of the casting solvent on the morphology of poly(styrene-b-isoprene) diblock copolymer/magnetic nanoparticle mixtures. Langmuir 22, 1375–1378.
Patil, R.M., Shete, P.B., Thorat, N.D., Otari, S.V., Barick, K.C., Prasad, A., Ningthoujam, R.S., Tiwale, B.M., Pawar, S.H., 2014. Non-aqueous to aqueous phase transfer of oleic acid coated iron oxide nanoparticles for hyperthermia application. RSC Adv. 4, 4515–4522.
Petcharoen, K., Sirivat, A., 2012. Synthesis and characterization of magnetite nanoparticles via the chemical co-precipitation method. Mater. Sci. Eng. B 177, 421–427.
Prince, R.C., 2015. Oil spill dispersants: boon or bane? Environ. Sci. Technol. 49, 6376–6384.
Romero, I.C., Toro-Farmer, G., Diercks, A.-R., Schwing, P., Muller-Karger, F., Murawski, S., Hollander, D.J., 2017. Large-scale deposition of weathered oil in the Gulf of Mexico following a deep-water oil spill. Environ. Pollut. 228, 179–189.
Sakti, S.C.W., Wijaya, R.A., Indrasari, N., Fahmi, M.Z., Widati, A.A., Abdulloh, Nuryono, Chen, C.-H., 2021. Magnetic hollow buoyant alginate beads achieving rapid remediation of oil contamination on water. J. Environ. Chem. Eng. 9, 104935.
Sarcletti, M., Vivod, D., Luchs, T., Rejek, T., Portilla, L., Müller, L., Dietrich, H., Hirsch, A., Zahn, D., Halik, M., 2019. Superoleophilic magnetic iron oxide nanoparticles for effective hydrocarbon removal from water. Adv. Funct. Mater. 29, 1805742.
Scott, P.J., Penlidis, A., Rempel, G.L., Lawrence, A.D., 1994. Ethylene-vinyl acetate semi-batch emulsion copolymerization: Use of factorial experiments for process optimization. J. Polym. Sci. Part A Polym. Chem. 32, 539–555.
Shen, C., Li, Y., Wang, H., Meng, Q., 2017. Mechanically strong interpenetrating network hydrogels for differential cellular adhesion. RSC Adv. 7, 18046–18053.
Si, Y., Fu, Q., Wang, X., Zhu, J., Yu, J., Sun, G., Ding, B., 2015. Superelastic and superhydrophobic nanofiber-assembled cellular aerogels for effective separation of oil/water emulsions. ACS Nano 9, 3791–3799.
Singh, B., Kumar, S., Kishore, B., Narayanan, T.N., 2020. Magnetic scaffolds in oil spill applications. Environ. Sci. Water Res. Technol. 6, 436–463.
Song, P., Cui, J., Di, J., Liu, D., Xu, M., Tang, B., Zeng, Q., Xiong, J., Wang, C., He, Q., Kang, L., Zhou, J., Duan, R., Chen, B., Guo, S., Liu, F., Shen, J., Liu, Z., 2020. Carbon microtube aerogel derived from kapok fiber: an efficient and recyclable sorbent for oils and organic solvents. ACS Nano 14, 595–602.
Sun, H., Xu, Z., Gao, C., 2013. Multifunctional, ultra-flyweight, synergistically assembled carbon aerogels. Adv. Mater. 25, 2554–2560.
Takuma, K., Uemichi, Y., Sugioka, M., Ayame, A., 2001. Production of aromatic hydrocarbons by catalytic degradation of polyolefins over H-gallosilicate. Ind. Eng. Chem. Res. 40, 1076–1082.
Wang, G., Zhao, J., Wang, Guizhen, Zhao, H., Lin, J., Zhao, G., Park, C.B., 2020a. Strong and super thermally insulating in-situ nanofibrillar PLA/PET composite foam fabricated by high-pressure microcellular injection molding. Chem. Eng. J. 390, 124520.
Wang, H., Mi, X., Li, Y., Zhan, S., 2020b. 3D graphene-based macrostructures for water treatment. Adv. Mater. 32, 1806843.
Wu, J., Li, H., Wu, S., Huang, G., Xing, W., Tang, M., Fu, Q., 2014. Influence of magnetic nanoparticle size on the particle dispersion and phase separation in an ABA triblock copolymer. J. Phys. Chem. B 118, 140213144409001.
Wu, J., Wang, N., Wang, L., Dong, H., Zhao, Y., Jiang, L., 2012. Electrospun porous structure fibrous film with high oil adsorption capacity. ACS Appl. Mater. Interfaces 4, 3207–3212.
Wu, M., Huang, S., Liu, T., Wu, J., Agarwal, S., Greiner, A., Xu, Z., 2021. Compressible carbon sponges from delignified wood for fast cleanup and enhanced recovery of crude oil spills by joule heat and photothermal effect. Adv. Funct. Mater. 31, 2006806.
Wu, Z.-Y., Li, C., Liang, H.-W., Chen, J.-F., Yu, S.-H., 2013. Ultralight, flexible, and fire-resistant carbon nanofiber aerogels from bacterial cellulose. Angew. Chem. Int. Ed. 52, 2925–2929.
Wu, Z.-Y., Liang, H.-W., Chen, L.-F., Hu, B.-C., Yu, S.-H., 2016. Bacterial cellulose: a robust platform for design of three dimensional carbon-based functional nanomaterials. Acc. Chem. Res. 49, 96–105.
Yang, L., Wang, Z., Yang, L., Li, X., Zhang, Y., Lu, C., 2017. Coco peat powder as a source of magnetic sorbent for selective oil–water separation. Ind. Crops Prod. 101, 1–10.
Yim, U.H., Kim, M., Ha, S.Y., Kim, S., Shim, W.J., 2012. Oil spill environmental forensics: the Hebei spirit oil spill case. Environ. Sci. Technol. 46, 6431–6437.
Yu, O.H., Lee, H.-G., Shim, W.J., Kim, M., Park, H.S., 2013. Initial impacts of the Hebei Spirit oil spill on the sandy beach macrobenthic community west coast of Korea. Mar. Pollut. Bull. 70, 189–196.

Yuan, X., Chung, T.C.M., 2012. Novel solution to oil spill recovery: using thermodegradable polyolefin oil superabsorbent polymer (Oil–SAP). Energy Fuels 26, 4896–4902.
Zhang, G., Nam, C., Chung, T.C.M., Petersson, L., Hillborg, H., 2017. Polypropylene copolymer containing cross-linkable antioxidant moieties with long-term stability under elevated temperature conditions. Macromolecules 50, 7041–7051.
Zhang, G., Nam, C., Petersson, L., Jämbeck, J., Hillborg, H., Chung, T.C.M., 2018. Increasing polypropylene high temperature stability by blending polypropylene-bonded hindered phenol antioxidant. Macromolecules 51, 1927–1936.
Zhu, K., Shang, Y.-Y., Sun, P.-Z., Li, Z., Li, X.-M., Wei, J.-Q., Wang, K.-L., Wu, D.-H., Cao, A.-Y., Zhu, H.-W., 2013. Oil spill cleanup from sea water by carbon nanotube sponges. Front. Mater. Sci. 7, 170–176.
Zhu, Q., Tao, F., Pan, Q., 2010. Fast and selective removal of oils from water surface via highly hydrophobic core−shell Fe_2O_3@C nanoparticles under magnetic field. ACS Appl. Mater. Interfaces 2, 3141–3146.